Solar Physics
DOI: 10.1007/•••••-•••-•••-••••-•

Investigation of quasi-periodic variations in hard X-rays of solar flares. II. Further investigation of oscillating magnetic traps

J. Jakimiec · M. Tomczak

© Springer ••••

arXiv:1103.3165v1 [astro-ph.SR] 16 Mar 2011

Abstract In our recent paper (Solar Physics **261**, 233) we investigated quasi-periodic oscillations of hard X-rays during impulsive phase of solar flares. We have come to conclusion that they are caused by magnetosonic oscillations of magnetic traps within the volume of hard-X-ray (HXR) loop-top sources. In the present paper we investigate four flares which show clear quasi-periodic sequences of HXR pulses. We also describe our phenomenological model of oscillating magnetic traps to show that it can explain observed properties of HXR oscillations. Main results are the following:

1. We have found that low-amplitude quasi-periodic oscillations occur before impulsive phase of some flares.
2. We have found that quasi-period of the oscillations can change in some flares. We interpret this as being due to changes of the length of oscillating magnetic traps.
3. During impulsive phase a significant part of the energy of accelerated (non-thermal) electrons is deposited within the HXR loop-top source.
4. Our analysis suggests that quick development of impulsive phase is due to feedback between pulses of the pressure of accelerated electrons and the amplitude of magnetic-trap oscillation.
5. We have also determined electron number density and magnetic filed strength for HXR loop-top sources of several flares. The values fall within the limits of $N \approx (2-15) \times 10^{10}$ cm^{-3}, $B \approx (45-130)$ gauss.

Keywords: Flares, Energetic Particles, Impulsive Phase, Oscillations

1. Introduction

In hard X-ray (HXR) emission of many flares quasi-periodic variations were observed with time-intervals between pulses, $P \sim 10-60$ s [see Lipa (1978) ; see also review of Nakariakov & Melnikov (2009) and references therein].

Astronomical Institute, University of Wrocław, ul. Kopernika 11, 51-622 Wrocław, Poland, email: jjakim;tomczak@astro.uni.wroc.pl

In our previous paper (Jakimiec & Tomczak, 2010, Paper I) we attempted to investigate relationship between HXR loop-top (LT) sources and the quasi-periodic variations. Main difficulty was that sequences of pulses are usually short, so that it is difficult to carry out comprehensive analysis of their quasi-periodicity. Therefore we used time-interval, Δt, between the strongest pulses as a simple estimate of the quasi-period P.

In the present paper we have selected four flares which have longer sequences of HXR pulses, so that it was possible to carry out detailed analysis of their quasi-periodicity (Section 2.1). Section 2.2 contains detailed analysis of 16 January 1994 flare. In Section 2.3 we estimate values of electron density and magnetic field strength inside several HXR loop-top sources. Section 3 contains discussion and conclusions.

2. Observations and their analysis

We used HXR observations recorded by *Yohkoh* Hard X-ray Telescope, HXT, (Kosugi *et al.*, 1991) [light-curves and images] and *Compton Gamma Ray Observatory* Burst and Transient Source Experiment, BATSE, (Fishman *et al.*, 1992) [light-curves].

2.1. Analysis of quasi-periodicity of HXR pulses

We have selected four flares which have longer sequences of HXR pulses, so that detailed analysis of their quasi-periodicity was possible. Main difficulty in the analysis was the fact that during impulsive phase the pulses occur simultaneously with quick increase of total HXR intensity (see Figure 1a). Therefore we have applied a method of normalization which is commonly used by radioastronomers (see Fleishman *et al.*, 2008). A normalized time series, $S(t)$, is:

$$S(t) = \frac{F(t) - \hat{F}(t)}{\hat{F}(t)}, \tag{1}$$

where $F(t)$ is the measured HXR flux and $\hat{F}(t)$ is a running average of $F(t)$. The red line in Figure 1a shows $\hat{F}(t)$ calculated with averaging time $\delta t = 30\,\mathrm{s}$. The normalized time series, $S(t)$ is shown in Figure 1b. Quasi-periodicity of the pulses is clearly shown in this Figure and it is confirmed by power spectrum seen in Figure 1c (Fourier transform of $S(t)$). The power spectrum has been calculated for time-interval 22:01-22:05:20 UT (Impulsive Phase, IP).

We see in Figures 1a and 1b that before the impulsive phase, between 21:58:40 and 22:00:20 UT, three increasing pulses occurred. Mean time-interval between the pulses is about 31 s which is close to the quasi-period, P, seen in the power spectrum (28 s). This suggests that these pulses also belong to the quasi-periodic sequence seen during impulsive phase.

Figure 2 shows a HXR light-curve of 16 January 1994 flare. Like in Figure 1a, during impulsive phase we see a sequence of increasing pulses. The red line connects tops of the pulses to show their quick non-linear increase and saturation.

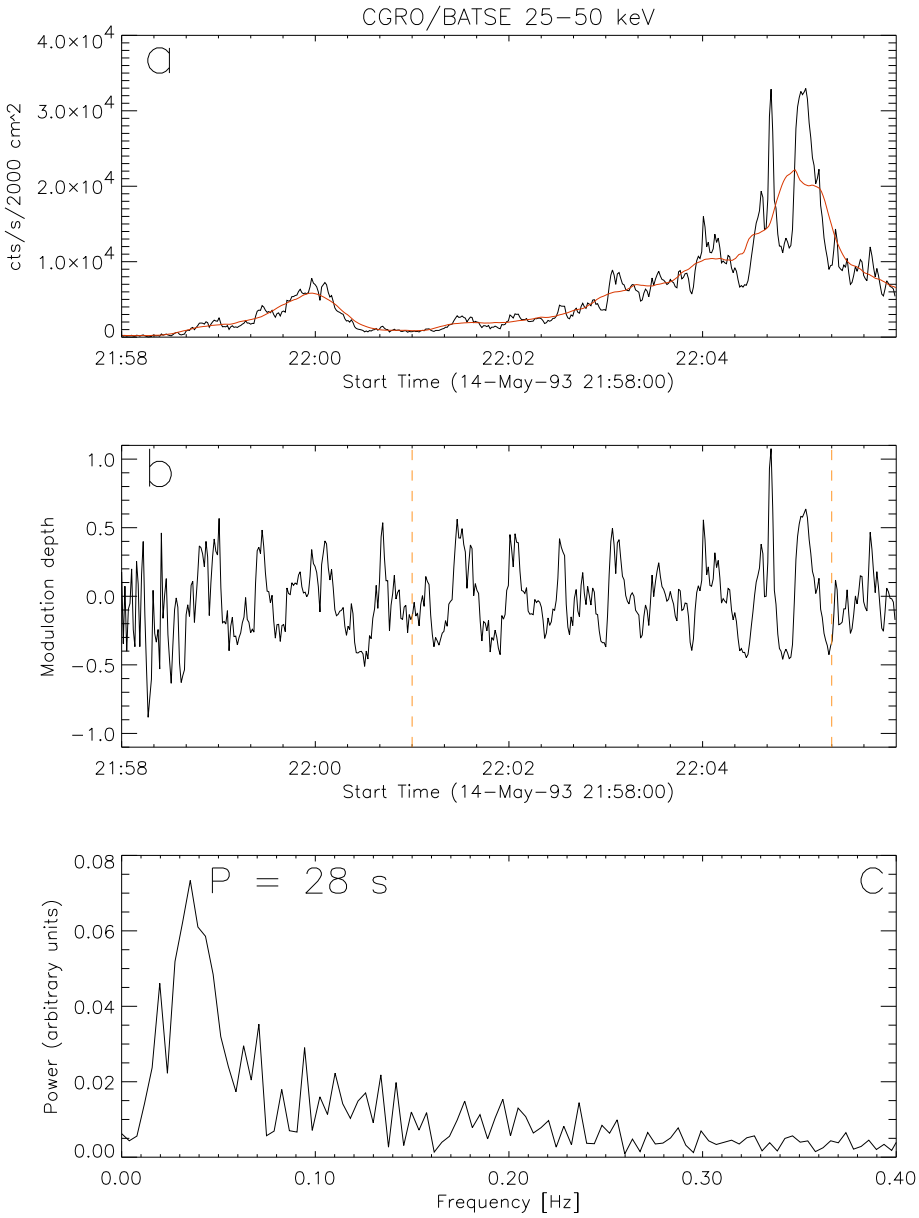


Figure 1. Analysis of the HXR light-curve (25-50 keV, *Compton Gamma Ray Observatory*/BATSE observations) for a flare of 14 May 1993. (a) HXR light-curve. The red line shows running average calculated with averaging time $\delta t = 30$ s. (b) Normalized light-curve, $S(t)$ [see Equation (1)]. Vertical dashed lines show the time-interval which was used to calculate power spectrum. (c) Power spectrum calculated for the normalized light-curve, $S(t)$. P is the period corresponding to the peak in power spectrum.

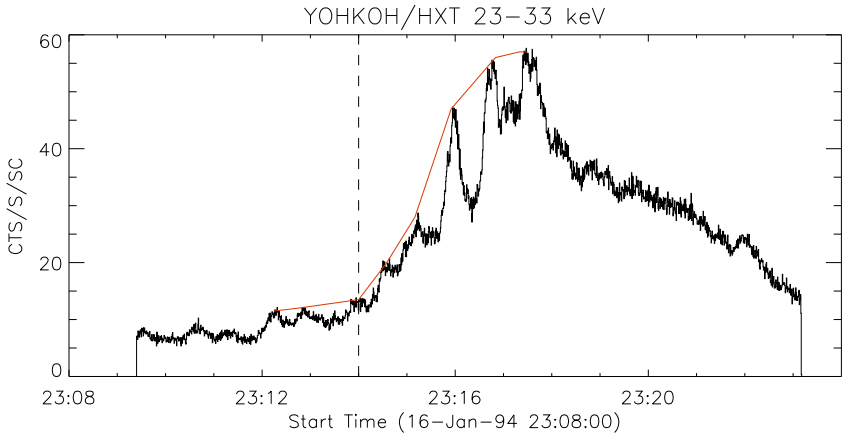


Figure 2. 23-33 keV light-curve recorded by *Yohkoh*/ Hard X-ray Telescope for a flare of 16 January 1994. The red line connects peaks of HXR pulses to visualize their non-linear increase and saturation. The noise is due to statistical fluctuations of counting rate. The dashed vertical line shows the beginning of impulsive phase.

Before the impulsive phase (BIP) there is a sequence of weak pulses. Normalization and power-spectrum analysis is shown in Figure 3. The power spectrum in Figure 3c has been calculated for time interval A, i.e. BIP plus IP. Figure 3d shows power spectrum calculated for the decay phase (time-interval B), where the pulses were weak and their profiles were disturbed, but the quasi-period had been retained.

Figure 4 shows HXR light-curve of 18 August 1998 flare. Its characteristic feature is that quasi-period during increase of HXR emission is shorter than during decrease of the emission. Therefore analysis of the light-curve has been done separately for time-intervals A and B (see Figures 5 and 6). In our model of oscillating magnetic traps changes of quasi-period are explained as being due to changes of length of oscillating traps (see Section 3).

Figure 7 shows HXR light-curves of 12 March 1993 flare. General behavior is similar to that seen in Figure 2: There are low-amplitude oscillations before impulsive phase and quick increase of HXR emission after the onset of impulsive phase. Specific feature are short-period oscillations after HXR maximum. Therefore analysis of the light-curve has been done separately for time-intervals A and B (see Figures 8 and 9). Change of the quasi-period is clearly seen.

2.2. Analysis of 16 January 1994 flare

We have chosen the flare of 16 January 1994 for further analysis because loop-top and footpoint sources can be easily recognized in its HXR images (Figure 10). We wanted to investigate what happened in the loop-top source during transition from low-amplitude oscillations to quick increase of HXR emission seen in Figures 2 and 3. Toward this end we have reconstructed *Yohkoh*/HXR images in energy channels L (14-23 keV), M1 (23-33 keV), and M2 (33-53 keV)

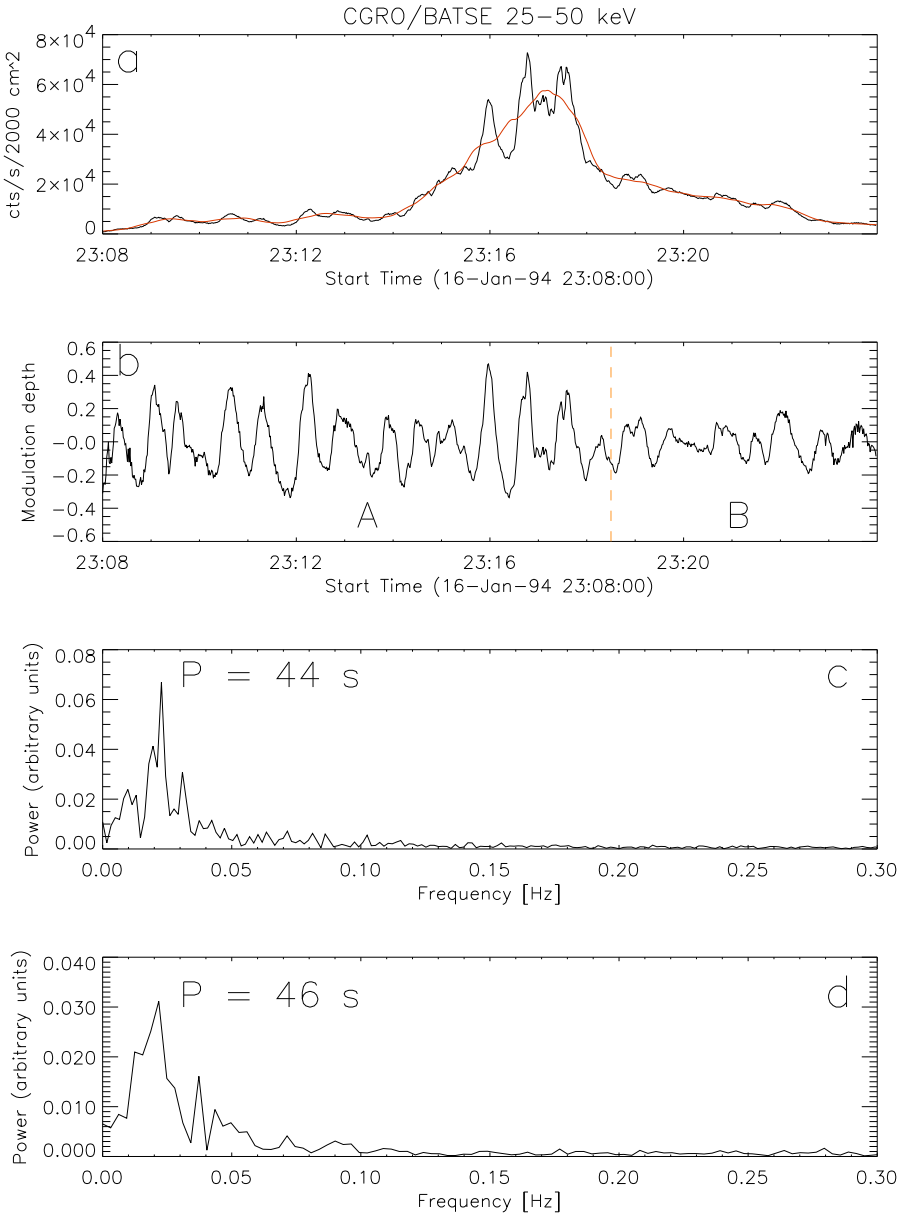


Figure 3. The same as in Figure 1, for a flare of 16 January 1994. the power spectra have been calculated for time intervals A and B and they are shown in panels (c) and (d).

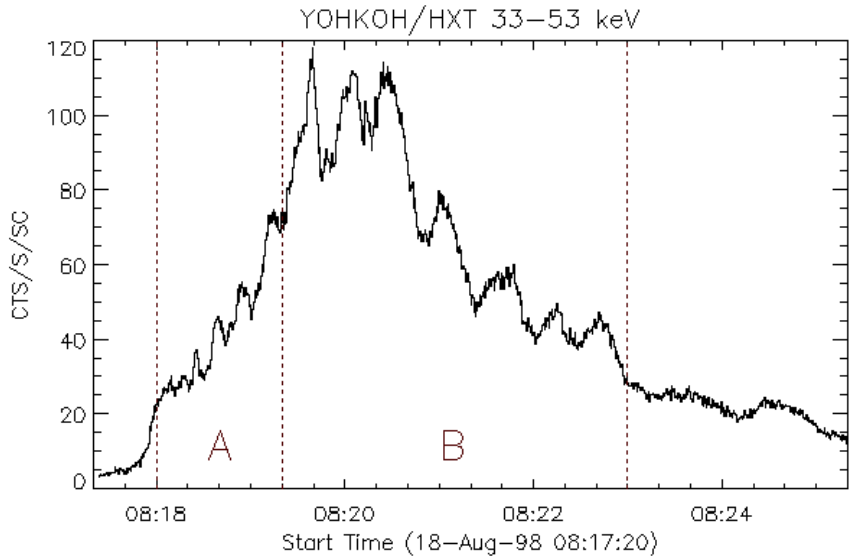


Figure 4. 33-53 keV *Yohkoh*/HXT light-curve for a flare of 18 August 1998. Power spectrum analysis has been carried out for time intervals A and B, separately, and results are presented in Figures 5 and 6.

for the time of Before Impulsive Phase (BIP) oscillations (upper row in Figure 10), about the beginning of impulsive phase (middle row) and for maximum of IP (lower row).

We see that before impulsive phase HXR footpoints are strong which means that accelerated electrons easily escape from the LT source. But at the beginning of impulsive phase the footpoints are weaker than the loop-top source (F < LT) in 14-23 and 23-33 keV emission which indicates that most of accelerated electrons deposit their energy within the LT source.

Next we have determined mean temperature, T, emission measure, EM, and mean electron number density, N, in the HXR LT source, from its *Yohkoh* soft-X-ray (SXR) images, using filter-ratio method (from Be119 and Al12 images). This analysis has been done in the following way: We have integrated SXR fluxes from area $A = 4$ *Yohkoh* pixels [i.e. 4.9×4.9 (arcsec)^2] at the center of HXR LT source. Next we determined diameter, d, of the HXR source according to isocontour $0.5I_{max}$, where I_{max} is the maximum intensity within the source. We assumed that extension of the HXR source along the line of sight is also d and calculated the volume of the emitting plasma as $V = 1.15Ad$ (here 1.15 is a correction factor which takes into account that actual size of the HXR source is somewhat larger than that determined from isocontour $0.5I_{max}$). Mean electron number density was calculated as $N = \sqrt{EM/V}$ and obtained time-variation of the temperature, $T(t)$, and density, $N(t)$, are shown in Figures 11 and 12.

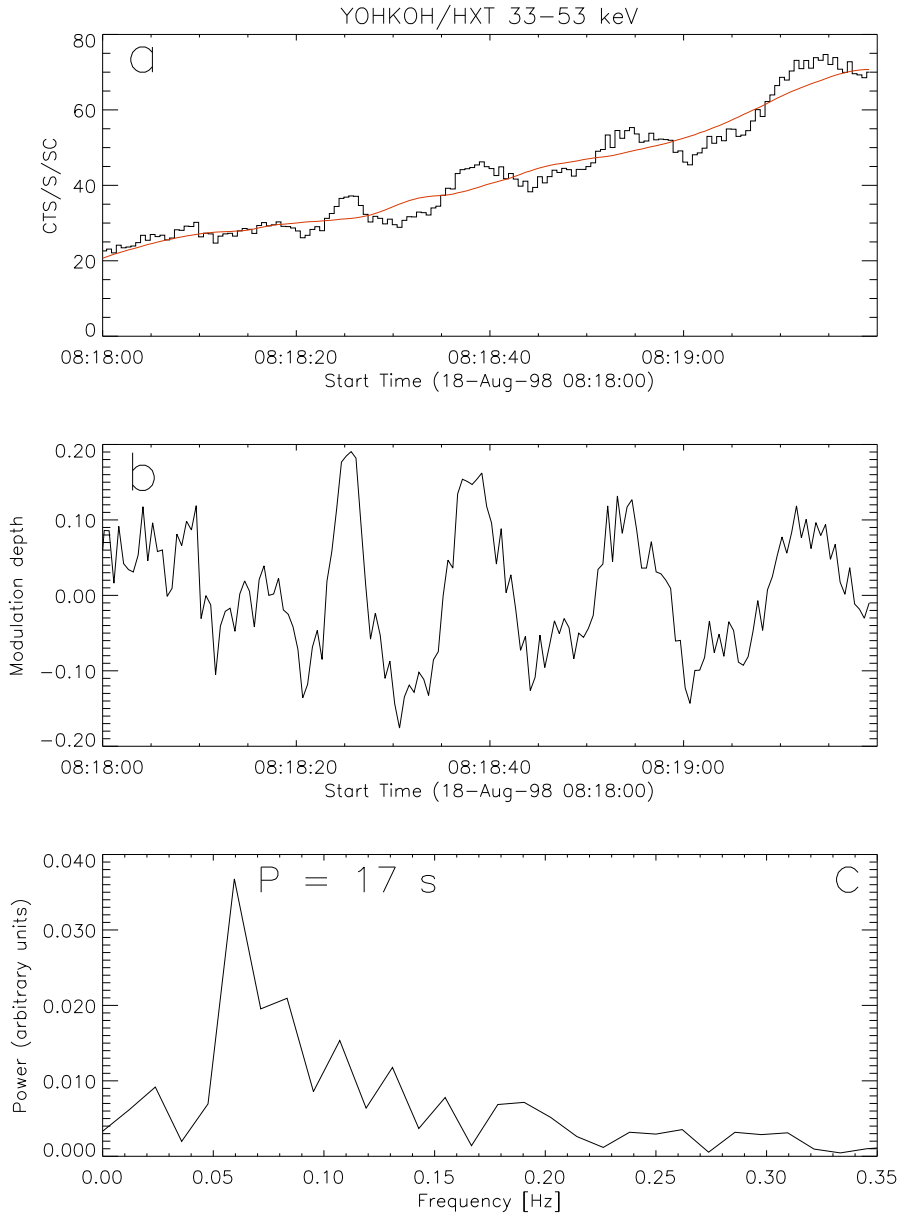


Figure 5. Power spectrum analysis for time-interval A of the flare of 18 August 1998.

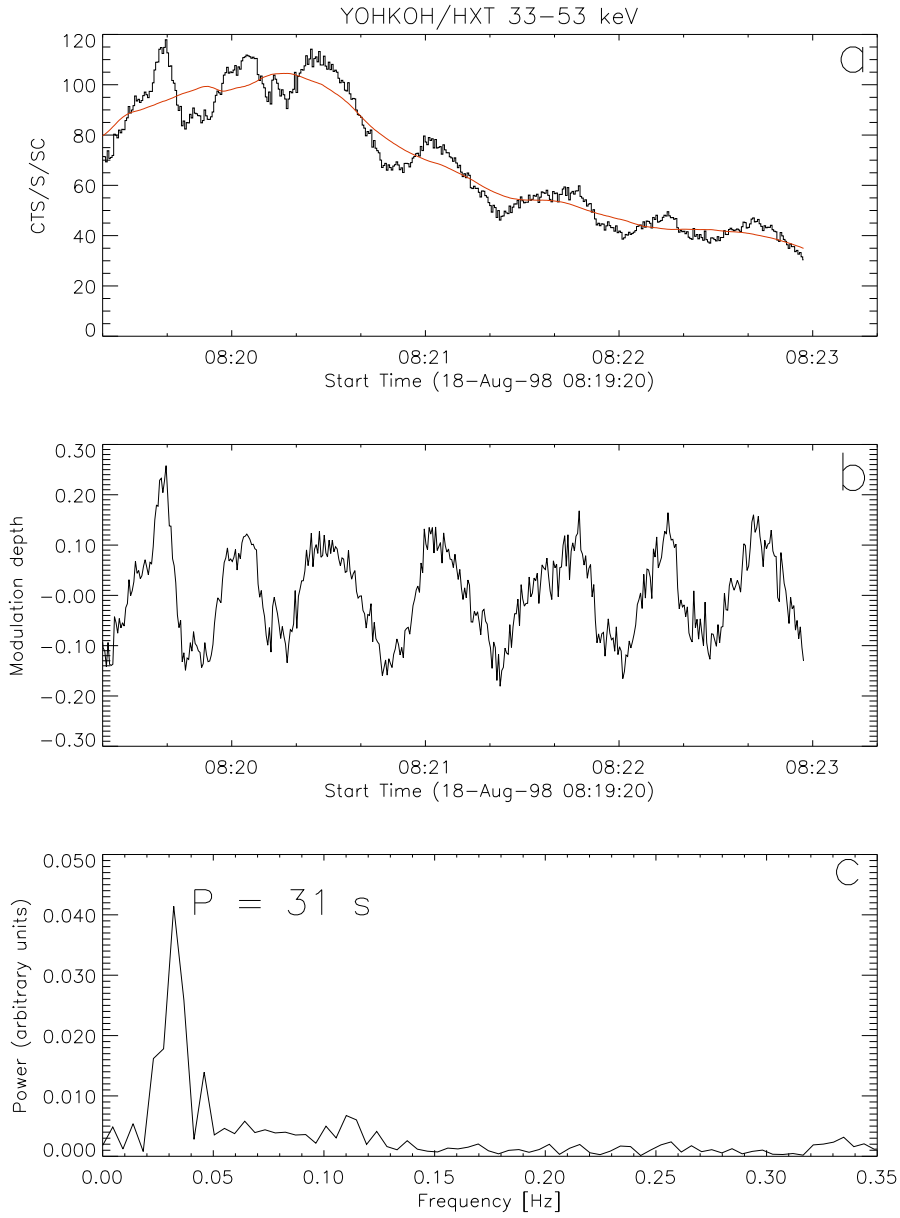


Figure 6. Power spectrum analysis for time-interval B of the flare of 18 August 1998.

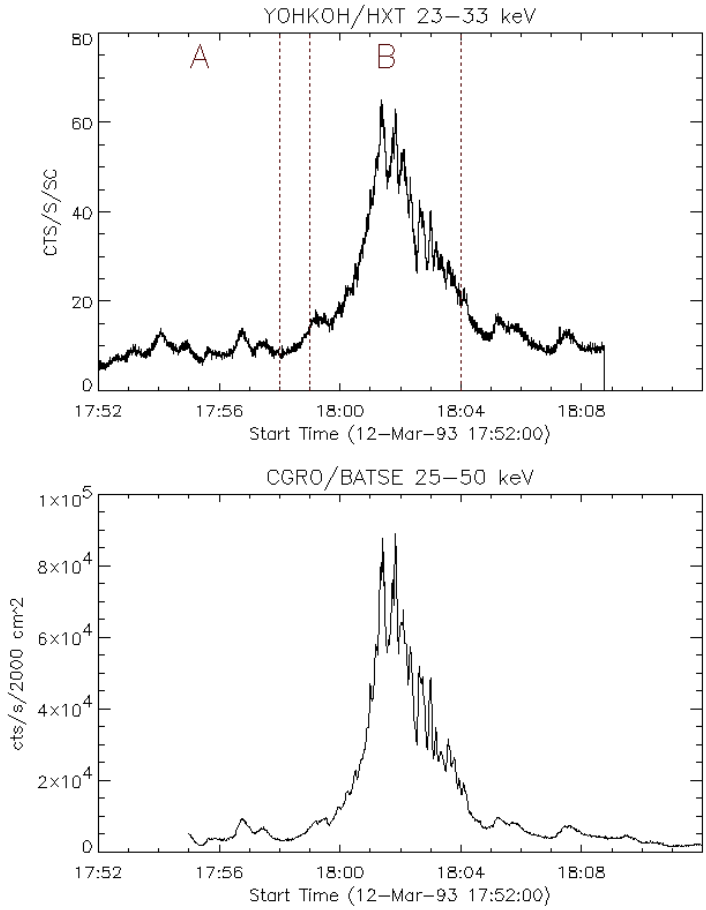


Figure 7. HXR light-curves for a flare of 12 March 1993 recorded by *Yohkoh*/HXT and *CGRO*/BATSE. Very good agreement of the fluctuations in both curves is seen. Power spectrum analysis has been carried out for time-intervals A and B which are marked by vertical lines.

Figure 11 shows that increase of energy release in the LT source began already about 23:10:40 UT. Sharp peaks of temperature about 23:12:30 and 23:16 UT (Figure 11) are correlated with peaks in HXRs (Figure 3b) which confirms that significant part of the energy of accelerated electrons is deposited within the loop-top source (the temperature peaks are somewhat, ∼16 s, delayed relative to the HXR peaks which is due to accumulation of plasma heating by accelerated electrons). Significant random fluctuations of $N(t)$ in Figure 12 are mostly due to random errors in estimates of the source volume from individual HXR images. Systematic increase of density with time seen in Figure 12 is due to chromospheric evaporation flow.

X-ray images for a flare of 30 October 1992 are shown in Figure 13. We see similar behavior like in Figure 10: Footpoint sources were stronger than LT

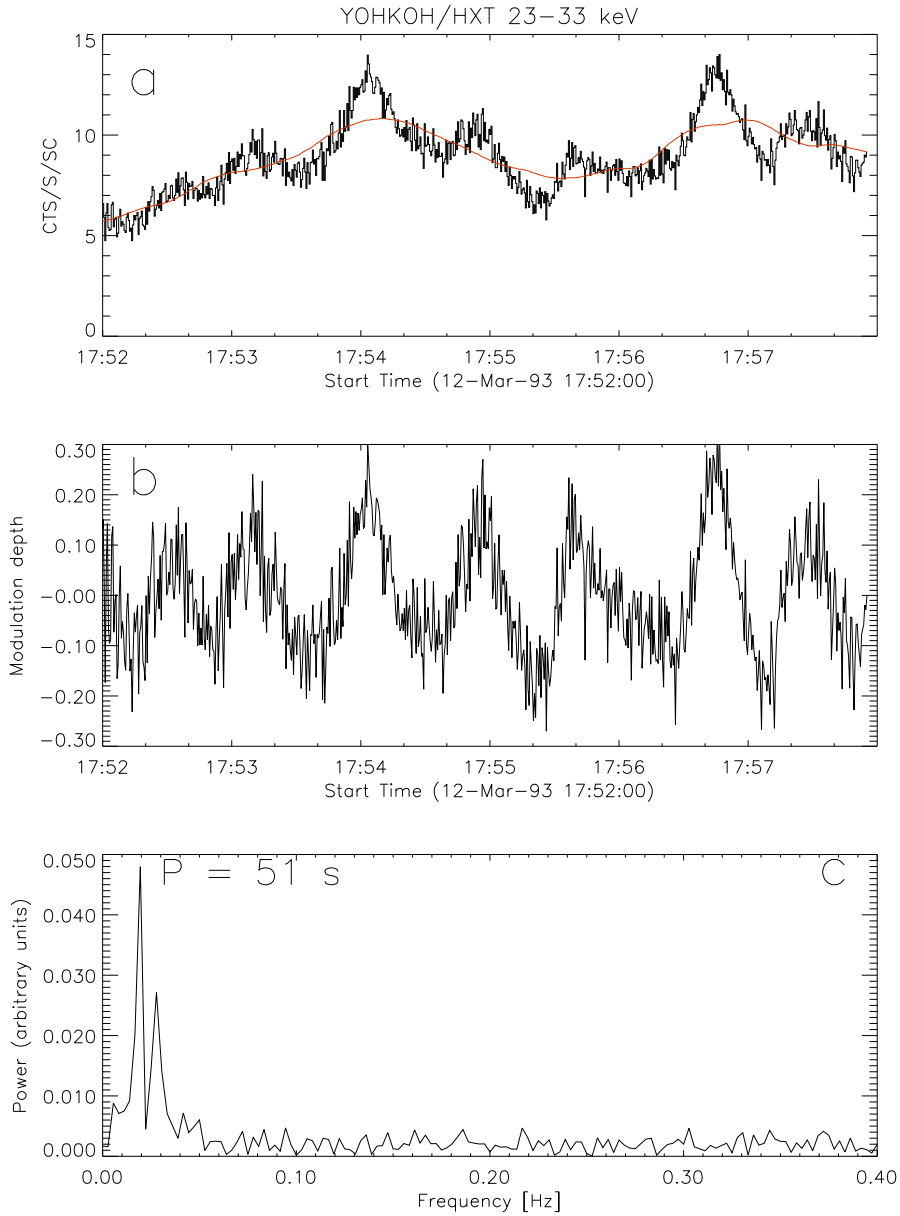


Figure 8. Power spectrum analysis for time-interval A of the flare of 12 March 1993.

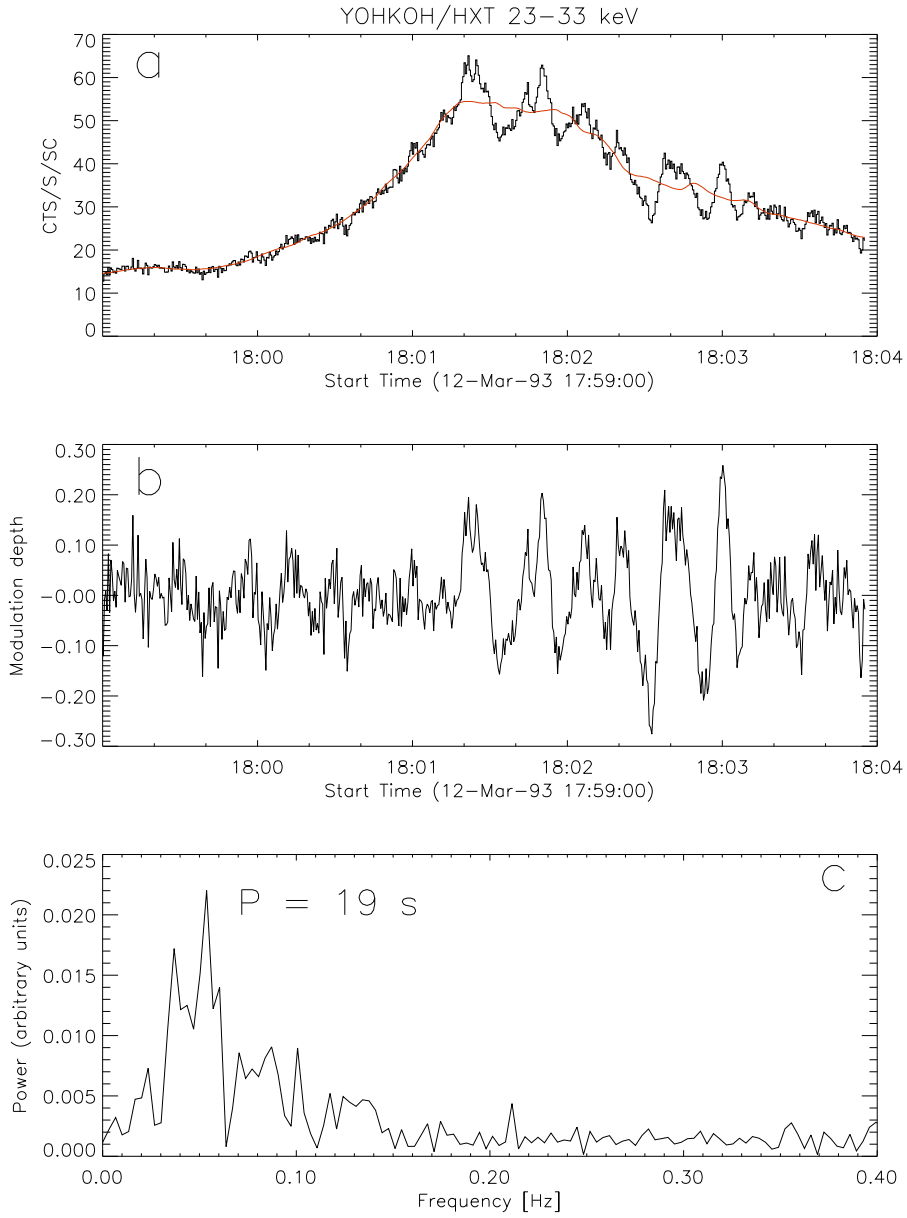


Figure 9. Power spectrum analysis for time-interval B of the flare of 12 March 1993.

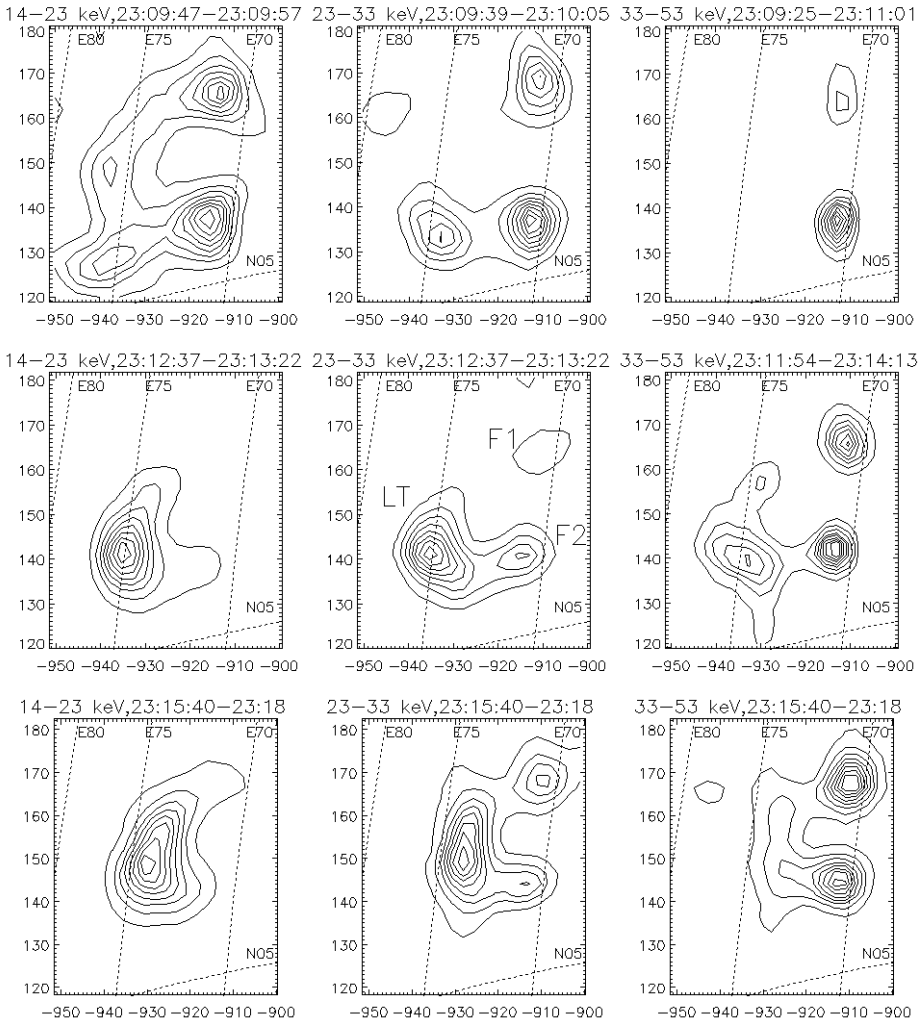


Figure 10. HXR images of the flare of 16 January 1994 in three energy channels: 14-23, 23-33, and 33-53 keV (vertical columns). Upper row: images recorded before impulsive phase, middle row: recorded near the beginning of impulsive phase, lower row: recorded during impulsive phase. See text for discussion.

source before impulsive phase and the LT source was stronger during impulsive phase.

2.3. Determination of magnetic field strength and electron densities for flares which were investigated in Paper I

In Paper I we used $N = 1.0 \times 10^{10}$ cm^{-3} as typical value of the electron number density in HXR LT sources during impulsive phase. This value has been obtained

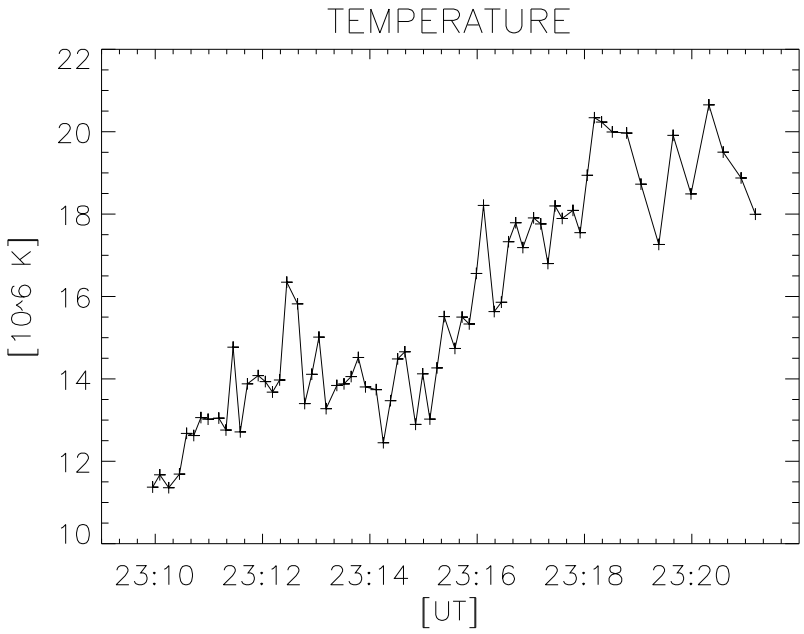


Figure 11. Time-variation of the mean temperature in HXR loop-top source of 16 January 1994 flare.

by Krucker and Lin (2008) from *RHESSI* soft-X-ray images of the sources. In Paper I we used this value of N to estimate magnetic field strength in oscillating magnetic traps:

$$B_2 = v_2\sqrt{4\pi\rho} \tag{2}$$

where v_2 is the wave speed estimated from analysis of HXR oscillations and $\rho \approx Nm_H$, m_H is the mass of proton. Obtained values of B_2 are given in Table 1.

For eight flares of those investigated in Paper I it was possible to determine mean electron density, N, for HXR LT source from SXR images using the method described in Section 2.2. The values are given in Table 1. We see that most values are significantly higher than that assumed in Paper I ($N = 1.0 \times 10^{10}$ cm^{-3}). This indicates that the value of N used in Paper I, and therefore also magnetic field strength, B_2, were underestimated. We have calculated corrected values, B_2^*, of the magnetic field strength using Equation (2) with the new values of N (see Table 1).

Let us note that values of electron number density, N, derived from *Yohkoh*/SXT images are reliable, since:

1. They have been confirmed by independent method (see Bak-Steślicka & Jakimiec, 2007),

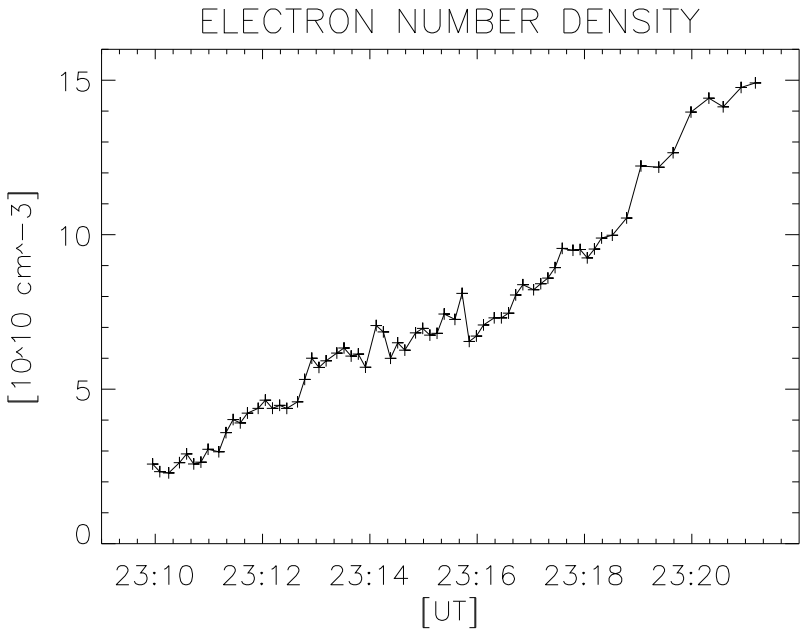


Figure 12. Time-variation of the mean electron number density in HXR loop-top source of 16 January 1994 flare.

2. Determination of N from *Yohkoh*/Al12 images does not depend significantly on temperature estimates, since instrumental response function for the Al12 images is nearly constant in wide range of temperatures (7-40 MK – see curve *f* in Figure 9 of Tsuneta *et al.*, 1991).

3. Discussion and summary

In Paper I we have proposed a model of oscillating magnetic traps to explain quasi-periodic oscillations seen in HXRs. In this model we have assumed that:

1. Magnetic structure at the top of flaring loop is triangular ("cusp-like"; Figure 14).
2. Electrons are efficiently accelerated during compression of magnetic traps (Somov and Kosugi, 1997, Karlický & Kosugi, 2004, Bogachev and Somov, 2005).

The cusp-like structure is now a standard model of solar flare magnetic field – see Aschwanden (2004) . At the top of this structure (near P in Figure 14) magnetic reconnection occurs. Reconnected magnetic field and plasma flow into the confined volume BPC with high velocity. Hence, it seems to be obvious that, this should excite magnetosonic oscillations within the BPC volume.

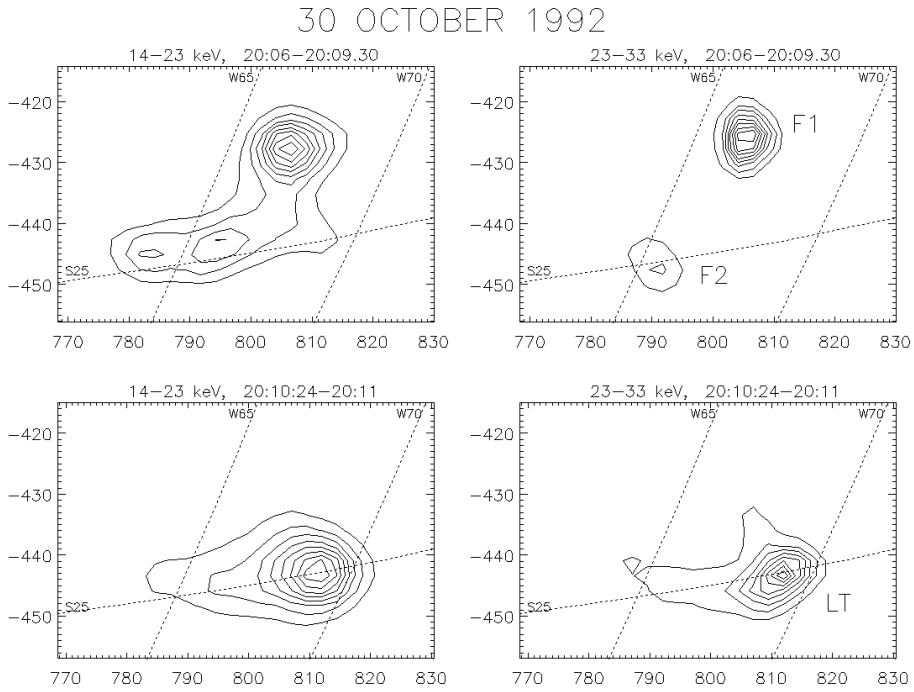


Figure 13. HXR images of the flare of 30 October 1992 in two energy channels: 14-23 and 23-33 keV (vertical columns). Upper row: images recorded before impulsive phase, lower row: images recorded during impulsive phase.

Table 1. Values of mean electron density and magnetic field strength

Date	UT	B_2 [G][a]	N [10^{10} cm^{-3}][b]	B_2^* [G][c]
28 Jun 92	14:00	36	1.6	45
8 May 98	01:59	40	2.3	62
31 Oct 91	09:11	26	6.0	64
14 May 93	22:05	30	12	104
7 Jun 93	14:22	33	15	127
16 Jan 94	23:17	35	8.0	98
23 Jun 00	14:26	28	15	61
25 Nov 00	18:39	21	9	63

[a] magnetic field strength estimated in Paper I (assuming $N = 1 \times 10^{10}$ cm^{-3})

[b] mean electron number density in HXR LT source at HXR maximum, estimated in the present paper

[c] magnetic field strength calculated with the new value of N

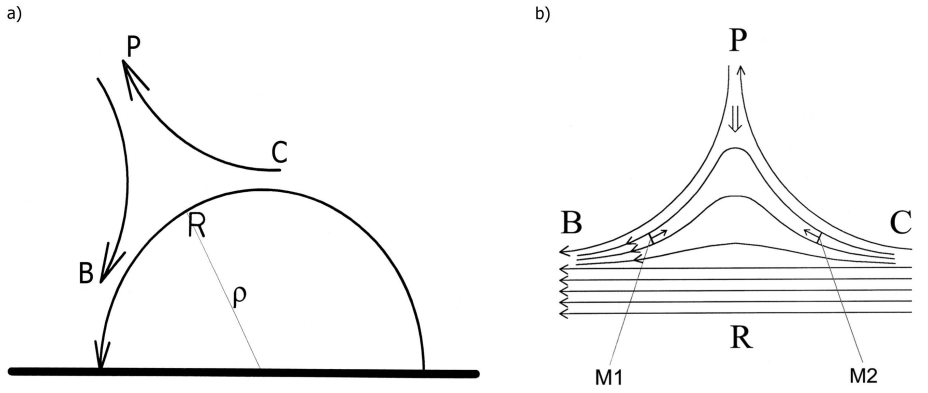


Figure 14. **a** Schematic diagram showing a cusp-like magnetic configuration. Magnetic fields PB and CP reconnect at P. The thick horizontal line is the chromosphere. **b** Detailed picture of the BPC cusp-like magnetic structure.

Magnetic fields PB and PC reconnect at P (Figure 14a). This generates a sequence of magnetic traps which move downward, the traps overtake each other, they collide and undergo compression (Figure 14b). During the compression particles are accelerated within the traps, magnetic pressure, gas pressure, and the pressure of accelerated particles increase, so that the compression is stopped, the traps can expand and undergo magnetosonic oscillations.

During the compression parameters of the traps undergo strong changes. At the beginning of compression the trap ratio, $\chi = B_{max}/B_{min}$, is high (B_{max} is the magnetic field strength at magnetic mirrors and B_{min} is the strength at the middle of the trap). The trap ratio decreases during compression and it reaches the lowest value, χ_{min}, at the end of compression. Then the electrons reach highest energies and they can most easily escape from the trap. Plasma density determines the fraction of accelerated electrons which lose their energy within the trap, i.e. before they escape from the loop-top source. This fraction depends on the energy, since Coulomb losses depend on energy (see changes of the footpoint/loop-top intensity ratio along rows and along columns in Figure 10).

Distribution of the oscillations within the BPC volume is determined by the time-profile, $v(t)$, of the velocity of reconnection flow which excites the oscillations. Its central part ($dv/dt \approx 0$) determines a "main trap" which contains many electrons and which is responsible for strong HXR pulses. Wings of the velocity profile ($dv/dt \neq 0$) are responsible for excitation of oscillations of many other ("secondary") traps whose oscillations are shifted in phase. Superposition of many HXR pulses coming from these secondary traps gives a "quasi-smooth" emission (seen as the emission below the pulses in Figures 1-9). We see that this quasi-smooth emission is stronger than pulses in the investigated flares which indicates that most of the volume BPC was filled with the "secondary" traps (their volume was greater than the volume of main trap).

In many flares HXR pulses are not clearly seen during quick increase of HXR emission, i.e. during beginning of impulsive phase (see example in Figure 9). According to our model of oscillating magnetic traps, in such cases the time-profile, $v(t)$ of reconnection flow is quasi-rectangular, i.e. its maximum is flat. Therefore, it excites many oscillating traps of similar power, which have different length (see Figure 14b) and their oscillations are shifted in phase. This gives strong quasi-smooth HXR emission. Clear quasi-periodic pulses are seen only near maximum of HXR emission (see Figure 9).

When we observe a long sequence of quasi-periodic oscillations (like in Figures 1-9), this indicates that:

1. The oscillations have been excited by a short pulse of reconnection flow (otherwise the oscillations would be more chaotic).
2. The oscillations are self-maintained, i.e. some feedback mechanism operates which causes that the oscillations do not decay, but they increase during impulsive phase.

Krucker and Lin (2008) investigated HXR LT sources from *RHESSI* observations and they have found that the energy contained in non-thermal electrons is usually higher than thermal energy. This means that also the pressure of non-thermal electrons is higher than gas pressure, $p_{NT} > p$. This suggests that the pressure, p_{NT}, of non-thermal electrons is an important factor in the feedback mechanism which maintains the oscillations of magnetic traps. During compression of a magnetic trap the pressure p_{NT} steeply increases and this causes increase of the amplitude of next expansion of the trap. This, in turn, causes increase of restoring force (i.e. the tension of bent magnetic field lines) and therefore the pulse of the pressure p_{NT} will be stronger during the next compression. Hence, there is a feedback between the intensity of pulses of the pressure p_{NT} and the amplitude of the magnetic trap oscillation and this feedback is responsible for quick increase of the oscillations during impulsive phase.

It may be interesting to note that this mechanism of maintaining the oscillations is analogous to the mechanism of instability which is responsible for stellar pulsations ("non-adiabatic pulsations"): in both cases the point is that additional energy is accumulated during compression of the gas (it is the energy of helium ionization in the case of Cepheids and it is energy of non-thermal electrons in our case).

Main results of the present paper are the following:

1. It has been confirmed that quasi-periodic oscillations (QPO) occur in HXR emission of solar flares.
2. We have found that low-amplitude QPO occur before impulsive phase of some flares.
3. We have found that quasi-period of the oscillations can change in some flares. We interpret this as being due to changes of the length of oscillating magnetic traps.
4. During impulsive phase most of the energy of accelerated (non-thermal) electrons is deposited within the HXR loop-top sources (Section 2.2). [For weak HXR flares this is seen at lower energies (14-23 keV), but not at 23-33 keV.]

5. We argue that the basic properties of the HXR oscillations can be explained in terms of a simple model of oscillating magnetic traps (see Paper I). This model allows us also to explain large number of electrons which are accelerated during impulsive phase: Observations show that the amplitude of the oscillations quickly increases and therefore the traps are filled with increasing amount of plasma coming from chromospheric evaporation. This is main source of electrons which undergo acceleration.
6. We suggest that a feedback between the pressure of accelerated electrons and the amplitude of the following expansion of magnetic trap is the mechanism which causes the quick increase of the amplitude of oscillations.
7. We have also determined improved values of electron number density and magnetic field strength for HXR loop-top sources of several flares which were investigated in Paper I. Obtained values fall within the limits of $N \approx (2 - 15) \times 10^{10}$ cm^{-3}, $B \approx (45 - 130)$ gauss.

Main advantages of the model of oscillating magnetic traps are the following:

1. Acceleration of electrons occurs in a large volume (BPC in Figure 14).
2. During development of impulsive phase plasma is delivered into BPC volume by chromospheric evaporation flow whose density is higher than the density of surrounding corona. This explains why number of accelerated electrons is very high.

Acknowledgements The *Yohkoh* satellite is a project of the Institute of Space and Astronautical Science of Japan. The *Compton Gamma Ray Observatory* is a project of NASA. We would like to thank anonymous referee for valuable remarks which helped us to improve this paper. This work was supported by Polish Ministry of Science and High Education grant No. N N203 1937 33.

References

Aschwanden, M. J. 2004, *Physics of the Solar Corona. An Introduction*, Springer: Praxis
Bak-Steślicka, U., Jakimiec, J.: 2007, *Centr. Eur. Astrophys. Bull.*, **31**, 97.
Bogachev, S. A., Somov, B. V. 2005, *Astron. Letters*, **31**, 537
Fishman, G. J., Meegan, C. A., Wilson, R. B., Paciesas, W. S., & Pendleton, G. N.: 1992, in The Compton Observatory Science Workshop (NASA CP 3137), ed. C. R. Shrader, N. Gehrels, & B. Dennis (Grenbelt: GSFC), 26.
Fleishman, G. D., Bastian, T. S., Gary, D. E.: 2008, *Astrophys. J.*, **684**, 1433.
Jakimiec, J., Tomczak, M.: 2010, *Solar Phys.*, **261**, 233 (Paper I).
Karlický, M., Kosugi T. 2004, *Astron. Astrophys.*, **419**, 1159
Krucker, S., Lin, R. P.: 2008, *Astrophys. J.*, **673**, 1181.
Lipa, B. 1978, *Solar Phys.*, **57**, 191.
Kosugi, T., Makishima, K., Murakami, T., Sakao, T., Dotani, T., Inda, M., Kai, K., Masuda, S., Nakajima, H., Ogawara, Y., Sawa, M., Shibasaki, K.: 1991, *Solar Phys.*, **136**, 17.
Nakariakov, V. M., Melnikov, V. F.: 2009, *Space Sci. Rev.*, **149**, 119.
Somov, B. V., Kosugi, T. 1997, *Astrophys. J.*, **485**, 859
Tsuneta, S., Acton, L., Bruner, M., Lemen, J., Brown, W., Caravalho, R., Catura, R., Freeland, S., Jurcevich, B., Morrison, M., Ogawara, Y., Hirayama, T., Owens, J.: 1991, *Solar Phys.*, **136**, 37.